FULL PAPER

Dalton
www.rsc.org/dalton

Lithium complexes with a $[Cp^*{}_2Ti_2F_7]^-$ ligand: ^{19}F NMR probe for lithium solvation†

Andrej Pevec,[a] Franc Perdih,[a] Janez Košmrlj,[a] Barbara Modec,[a] Herbert W. Roesky[b] and Alojz Demšar *[a]

[a] *Faculty of Chemistry and Chemical Technology, University of Ljubljana, Aškerčeva 5, SI-1000 Ljubljana, Slovenia. E-mail: alojz.demsar@uni-lj.si; Fax: +386 1 2419 220; Tel: +386 1 2419 112*

[b] *Institut für Anorganische Chemie der Universität, Tammannstrasse 4, D-37077 Göttingen, Germany. E-mail: hroesky@gwdg.de; Fax: +49 551 39 3373; Tel: +49 551 39 3002*

Received 6th August 2002, Accepted 27th November 2002
First published as an Advance Article on the web 9th January 2003

Reaction of the *in situ* prepared lithium fluoride with $[Cp^*TiF_3]_2$ afforded $[\{Li(Cp^*{}_2Ti_2F_7)\}_2(THF)_2]\cdot 2THF$, **3**·2THF. The addition of 12-crown-4 to a THF solution of **3**·2THF results in $[\{Li(Cp^*{}_2Ti_2F_7)\}_2(\mu_2\text{-}\eta^1{:}\eta^1\text{-}12\text{-crown-}4)]\cdot$(12-crown-4), **4**·(12-crown-4). In the solid state structures of **3**·2THF and **4**·(12-crown-4), which consist of dimeric $[Li(Cp^*{}_2Ti_2F_7)]_2$ units, the lithium atom is coordinated by three fluorine atoms and an oxygen atom from the ether. Dimeric and monomeric (with respect to lithium) species were observed in solution of **3**·2THF or **4**·(12-crown-4). The solvation of the lithium atom in monomeric species $[Li(Cp^*{}_2Ti_2F_7)S_n]$ with S = $CDCl_3$, 12-crown-4, THF-d_8, was studied by variable temperature ^{19}F NMR spectroscopy. Slow exchange of coordinated deuterated trichloromethane and 12-crown-4 on lithium ion was observed in a $CDCl_3$/12-crown-4 solution of **4**·(12-crown-4) by ^{19}F NMR spectroscopy up to 302 K.

Introduction

The coordination of solvent molecules to the lithium cation strongly influences the structures of lithium halides, amides, imides, enolates, alkoxides, organolithium reagents, and their mixtures in the solid state as well as the structures and reactivity in solution.[1] The exchange of lithium-coordinated solvent molecules in solution at room temperature is very fast.[2] The rate of exchange is diminished at temperatures close to the freezing points of solvents such as pentane, THF, diethyl and dimethyl ether, toluene, and their mixtures, thus making possible observation of lithium solvated species by NMR spectroscopy.[2] ^6Li, ^7Li, ^{13}C, ^{15}N and ^{31}P NMR spectroscopy have been used to study aggregation and solvation equilibria and their impact on reactivity.[1] The broad range of ^{19}F NMR chemical shifts makes this nucleus useful for NMR observation of species undergoing dynamics at a higher rate than accessible with ^6Li, ^7Li, ^{13}C, ^{15}N and ^{31}P nuclei.[3] The dissociation equilibrium of $[(Cp^*TiF_3)_4\text{-}LiF]$ **1** in solution has been observed by variable temperature ^{19}F NMR spectroscopy (Scheme 1).[4] In the present study, the $[Cp^*{}_2Ti_2F_7]^-$ ligand coordinated to the lithium ion served as a ^{19}F NMR probe for the solvation of the lithium cation by trichloromethane, THF and 12-crown-4. Solvated species were observed in slow exchange up to 302 K.

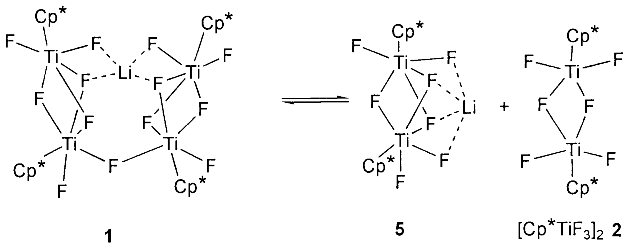

Scheme 1

Results and discussion

Synthesis and crystal structures

$[Cp^*TiF_3]_2$ **2** reacts with the *in situ* prepared lithium fluoride (formed by the reaction of trimethyltin fluoride and lithium chloride) in tetrahydrofuran solution. Crystals of dimeric $[\{Li(Cp^*{}_2Ti_2F_7)\}_2(THF)_2]\cdot 2THF$, **3**·2THF, were grown by slow evaporation of solvent at reduced pressure. The polymeric $[\{Li(Cp^*{}_2Ti_2F_7)\}_2(\mu_2\text{-}\eta^1{:}\eta^1\text{-}12\text{-crown-}4)]\cdot$(12-crown-4), **4**·(12-crown-4), crystallizes from a THF solution of **3**·2THF/12-crown-4 (molar ratio 1 : 4). The molecular structures of **3**·2THF (Fig. 1, Table 1) and **4**·(12-crown-4) (Scheme 2, Fig. 2, Table 2) consist of two $[Cp^*{}_2Ti_2F_7]^-$ ligands coordinated to two lithium ions in bidentate and monodentate fashion. The fourth coordination site of lithium ion is occupied by an oxygen atom from THF (in **3**·2THF) or 12-crown-4 (in **4**·(12-crown-4)). The Li-F distances in **3**·2THF and **4**·(12-crown-4) (1.799(5)–1.896(4) Å) are similar to those in tetracoordinated lithium in **1** (1.864(13)–1.932(12) Å)[4] and in $[Cp^*In(C_5H_3NO_2)_3]\cdot LiF$ (1.755(11) Å),[5] and are shorter than those in lithium fluoride

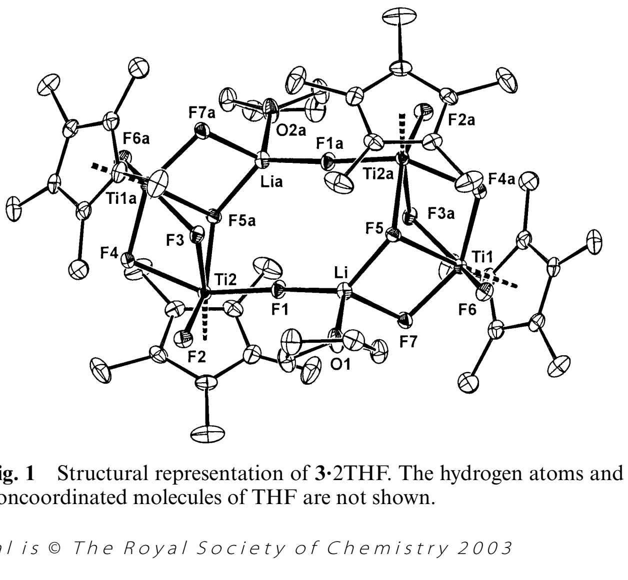

Fig. 1 Structural representation of **3**·2THF. The hydrogen atoms and noncoordinated molecules of THF are not shown.

DOI: 10.1039/b207685c

---

† Electronic supplementary information (ESI) available: optimised cartesian coordinates. See http://www.rsc.org/suppdata/dt/b2/b207685c/

Table 1 Selected bond distances (Å) and angles (°) for **3**·2THF

Li–F1	1.804(4)	Ti1–F3a	1.9757(12)
Li–F5	1.896(4)	Ti1–F4a	2.0168(12)
Li–F7	1.883(4)	Ti2–F1	1.8853(12)
Li–O1	1.931(4)	Ti2–F2	1.8403(13)
Ti1–F5	2.2503(12)	Ti2–F3	2.1425(12)
Ti1–F6	1.8388(12)	Ti2–F4	2.0338(12)
Ti1–F7	1.8831(12)	Ti2–F5a	2.0168(12)
F6–Ti1–F5	79.37(5)	F1–Li–F5	131.8(2)
F6–Ti1–F7	92.91(6)	F1–Li–F7	118.1(2)
F6–Ti1–F3a	146.40(5)	F1–Li–O1	106.14(18)
F6–Ti1–F4a	87.37(5)	Li–F1–Ti2	168.58(14)

Table 2 Selected bond distances (Å) and angles (°) for **4**·(12-crown-4)

Li–F1a	1.891(5)	Ti1–F4	2.0162(15)
Li–F5a	1.862(5)	Ti1–F5	2.2735(15)
Li–F7	1.799(5)	Ti2–F3	2.1466(15)
Li–O2	1.991(5)	Ti2–F4	2.0329(15)
Ti1–F1	1.8937(15)	Ti2–F5	2.0112(15)
Ti1–F2	1.8439(16)	Ti2–F6	1.8382(16)
Ti1–F3	1.9588(15)	Ti2–F7	1.8912(15)
F2–Ti1–F1	91.50(7)	F1a–Li–F5a	86.4(2)
F2–Ti1–F3	146.79(7)	F1a–Li–O2	107.5(2)
F2–Ti1–F4	87.14(7)	F5a–Li–O2	111.7(2)
F2–Ti1–F5	79.84(7)	Li–F7–Ti2	171.59(17)

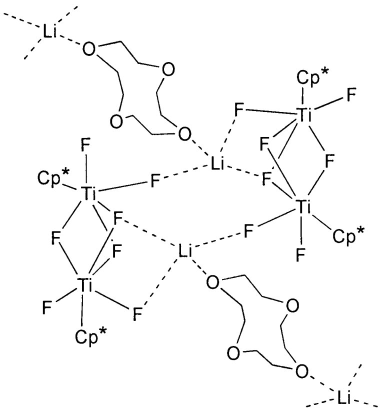

4

Scheme 2

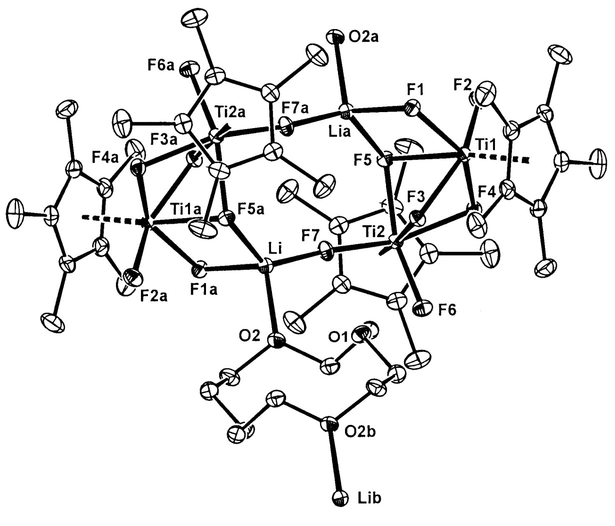

Fig. 2 Structural representation of **4**·12-crown-4. The hydrogen atoms and noncoordinated molecules of 12-crown-4 are not shown.

(2.009 Å).[6] The Ti–F distances of fluorines in the *trans* position to the Cp* ligand are longer than to other bridging fluorines. The Ti–F distances of lithium bonded fluorines are 0.05–0.09 Å longer than the others. The $[Li(Cp^*_2Ti_2F_7)]_2$ units in **4**·(12-crown-4) are connected into a chain by bridging 12-crown-4 molecules coordinated to two lithium ions in a η^1-fashion (Scheme 2).

The addition of 12-crown-4 to lithium inorganic and organic compounds has drawn a considerable interest in chemistry. The solid state and solution structures revealed the tetradentate ligation of 12-crown-4 to the lithium ion.[7] So far the η^1-coordination of 12-crown-4 to lithium has been only observed in $[Li_2(12\text{-crown-}4)_3]^{2+}$ cation where two 12-crown-4 moieties retain the common η^4-coordination, while the third 12-crown-4 molecule serves as a bridge between two lithium cations, coordinated to each in a η^1 mode.[8] Therefore the fluorine donating ligand $[Cp^*_2Ti_2F_7]^-$ in **4**·(12-crown-4) is the only known ligand that forces 12-crown-4 solely to the ether-like η^1-coordination on lithium.

Variable temperature (VT) NMR studies of 3·2THF and 4·(12-crown-4)

VT spectra of 3·2THF in THF-d_8. The variable temperature ^{19}F NMR spectra of **3**·2THF in THF-d_8 are shown in Fig. 3a–d.

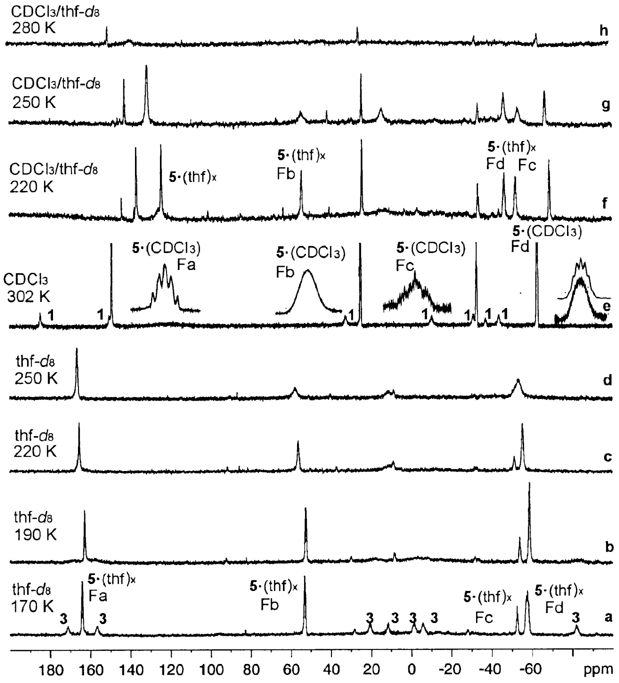

Fig. 3 Variable temperature ^{19}F NMR spectra of **3**·2THF at 282 MHz; (a–d) THF-d_8 (0.02M) solution, (e) $CDCl_3$ (0.02 M) solution, (f–h) 0.007 M $CDCl_3$/THF-d_8 (molar ratio 2.5 : 1) solution. The insets are resonances of **5**·$CDCl_3$, two F_d resonances shown are from samples of $[^6Li]$**3**·2THF (septet) and **3**·2THF (singlet).

The room temperature ^1H NMR spectrum of **3**·2THF shows a single Cp* resonance while the ^{19}F NMR resonances are broadened into the baseline. Cooling the solution to 170 K results in four sharp and seven broad fluorine resonances. With the temperature increased to 190 K, these seven resonances broaden into the baseline and at 220 K a new resonance appears at δ 10 ppm. Four sharp resonances do not broaden in the same manner in VT NMR spectra, as evident from the resonances at δ 162 and 52 ppm. The former broadens above 250 K, while the latter already broadens above 220 K.

These changes in the spectra can be explained by the processes depicted in Scheme 3. The set of seven broad resonances observed at 170 K is ascribed to the dimeric (with respect to lithium) molecule of **3**. The seven resonances are in agreement with the seven nonequivalent fluorine atoms, corresponding the centrosymmetric solid state structure of **3**·2THF. The four

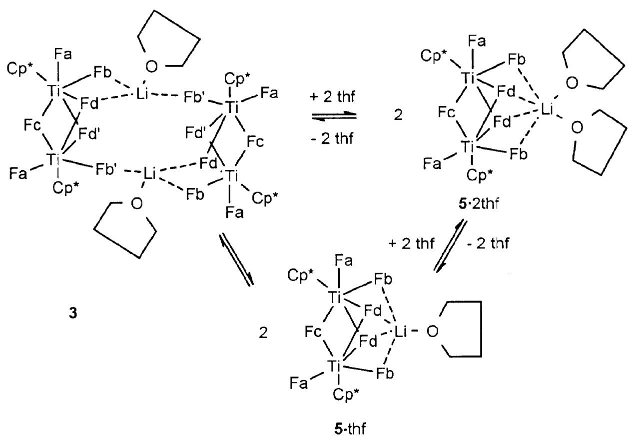

Scheme 3

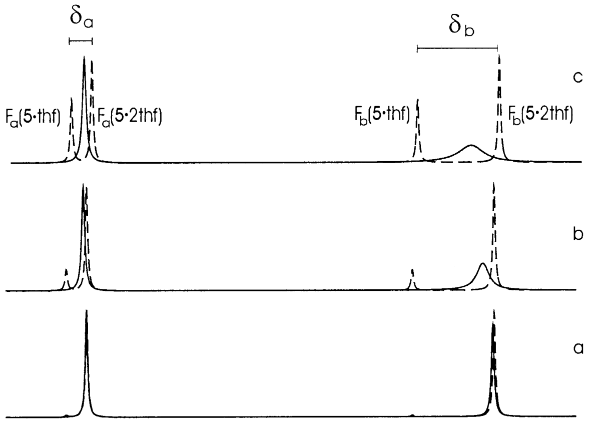

Fig. 4 Simulated spectra for the equilibrium **5**·2THF ↔ **5**·THF + THF in a slow exchange (dashed line) and at different rates k and **5**·THF/**5**·2THF ratios in a fast exchange (solid line). $\Delta\delta_a$ and $\Delta\delta_b$ (see text) are set to 0.5 and 2 ppm, respectively. (a) $k = 500\ \mathrm{s}^{-1}$, **5**·THF/**5**·2THF = 0.02, (b) $k = 1000\ \mathrm{s}^{-1}$, **5**·THF/**5**·2THF = 0.2, (c) $k = 2000\ \mathrm{s}^{-1}$, **5**·THF/**5**·2THF = 0.6.

sharp resonances with the intensity ratio of 2 : 2 : 1 : 2 are ascribed to the monomeric molecules of **5**·(THF)$_x$ and are in agreement with a bowl-like [Cp*$_2$Ti$_2$F$_7$]$^-$ ligand, coordinated to lithium by four donating fluorine atoms. Two of these resonances (for F$_b$ and F$_d$), appearing at lower frequencies than in Hdmpy[Cp*$_2$Ti$_2$F$_7$] (dmpy = 2,6-dimethylpyridine)[9a] or Me$_4$N[Cp*$_2$Ti$_2$F$_7$] [9b] are ascribed to the lithium-coordinated fluorine atoms. Similar low-frequency shift of metal-coordinated F$_b$ and F$_d$ resonances was observed in the spectra of [(Cp*$_2$Ti$_2$F$_7$)$_2$Ca] [10] and [(Cp*$_2$Ti$_2$F$_7$)$_3$La].[9a] The resonances of **3** are broadened due to dissociation equilibria giving monomeric molecules **5**·(THF)$_x$. With the increased dissociation rate at higher temperatures the resonances of **3** coalesce to the single resonance at δ 10 ppm (Fig. 3).

The broadening of F$_a$ (above 250 K) and F$_b$ (above 220 K) resonances in **5**·(THF)$_x$ at different temperatures can be rationalised as follows. Two species **5**·THF and **5**·2THF are present in the equilibrium. At a very low temperature this equilibrium would be shifted completely towards the thermodynamically more stable **5**·2THF (see the Theoretical calculations part below), resulting in a single F$_b$ resonance. At the elevated temperatures the concentration of monosolvated **5**·THF increases, accounted for by the entropical shift of the **5**·2THF ↔ **5**·THF + THF equilibrium. In these species lithium-coordinated fluorines F$_b$ are expected to resonate at two slightly different frequences ($\Delta\delta_b = |\delta_{(\mathrm{Fb\ in\ 5\cdot THF})} - \delta_{(\mathrm{Fb\ in\ 5\cdot 2THF})}|$), which, however, due to the rapid equilibration of **5**·THF and **5**·2THF appear as one single broad resonance. The smaller $\Delta\delta_a$ is expected, since the resonance of terminal F$_a$ is less effected by changes in lithium solvation due to the larger fluorine–lithium distance. The smaller $\Delta\delta_a$ results in the less pronounced resonance broadening as in the case of F$_b$. This model is confirmed by the simulation in Fig. 4.

VT NMR spectra of 3·2THF in CDCl$_3$ and in CDCl$_3$/THF-d_8. The ^{19}F NMR spectrum of **3**·2THF (CDCl$_3$ solution) shows four sharp fluorine resonances in the intensity ratio of 2 : 2 : 1 : 2 in the temperature range 222–312 K (spectrum at 302 K is shown in Fig. 3e). The resonances are ascribed to monomeric species **5**·(CDCl$_3$)$_x$. Two resonances of fluorine atoms non-bonded to lithium appear as a quintet (F$_a$) and a multiplet (F$_c$) (see insets in Fig. 3e). The F$_a$ quintet with the coupling constant of 44 Hz can be explained by coupling of F$_a$ to four proximal fluorine atoms. Two resonances of lithium-bonded fluorine atoms (F$_b$ and F$_d$) are singlets, decoupled presumably by the quadrupolar ^{7}Li nucleus. This assignment is in agreement with the fact that in structurally analogous [(Cp*$_2$-Ti$_2$F$_7$)$_2$Ca] calcium-bonded F$_b$ and F$_d$ appear as multiplets.[10b] On the other hand, CDCl$_3$ solution of [^{6}Li]**3**·2THF exhibits a septet-like F$_d$ resonance of **5**·(CDCl$_3$)$_x$ (separations of resonances are 48 Hz), with the other fluorine resonances being very similar to those in the solution of unlabelled **3**·2THF. The difference in the shape of F$_d$ resonance can be explained by different decoupling of fluorine resonances caused by ^{6}Li and ^{7}Li, having quadrupole moments of -6.4×10^{-32} m^2 and -3.7×10^{-30} m^2, respectively.[11] In contrast to F$_d$, the F$_b$ resonance of [^{6}Li] enriched **5**·(CDCl$_3$)$_x$ is a singlet. This can be rationalised by the dynamics of the lithium ion, equidistant from the pair of F$_d$ atoms, but slightly closer to one of both F$_b$, dancing (moving fast) between these two F$_b$ atoms. Due to the absence of the fine structure of the F$_d$ resonance and due to extensive coupling in **5**·(CDCl$_3$)$_x$ (C_2 symmetry, 16 coupling constants) we were unable to simulate **5**·(CDCl$_3$)$_x$ fluorine spectrum to determine ^{6}Li–^{19}F coupling.

It has been found that trichloromethane effectively solvates calcium ion in [{(C$_5$Me$_4$Et)$_2$Ti$_2$F$_7$}$_2$Ca], where the equilibrium of species with solvated and with non-solvated calcium ion (ΔH_{solv} of -19 kJ mol^{-1}) was monitored by ^{19}F NMR spectroscopy.[10] Similarly, the solvation of the lithium ion with CDCl$_3$ molecules is assumed for species **5**·(CDCl$_3$)$_x$. The sharp and temperature-independent shapes of resonances in the temperature range 222–312 K (spectrum at 302 K is shown in Fig. 3e) of CDCl$_3$ solution of **3**·2THF indicate the lack of equilibrium, previously discussed for the THF-d_8 solution. In this case the monosolvated form **5**·CDCl$_3$ is probably preferred, as expected on the basis of steric considerations. In addition to the four main fluorine resonances, a set of seven minor resonances (ratio 2 : 2 : 2 : 2 : 2 : 1 : 2) was observed in the temperature range 222–312 K (Fig. 3e for spectrum at 302 K). These belong to [(Cp*TiF$_3$)$_4$LiF] (**1**).[4] The resonances of **1** suggest partial decomposition of **5**·CDCl$_3$ to [Cp*TiF$_3$]$_2$ (**2**) and lithium fluoride, followed by the equilibrium reaction shown in Scheme 1, finally resulting in the tetratitanium molecule **1**. The CDCl$_3$ solution of **3**·2THF shows an additional fluorine resonance (δ -197 ppm) with an intensity close to that of the small resonances of **1**. This additional resonance has a line-width $w_{1/2}$ = 420 Hz, which in the case of [^{6}Li]**3**·2THF drops to 180 Hz. The approximate relation of coupling constants is $J(^7\mathrm{Li}–^{19}\mathrm{F})/J(^6\mathrm{Li}–^{19}\mathrm{F}) = \gamma(^7\mathrm{Li})/\gamma(^6\mathrm{Li}) = 2.64$ (magnetogyric ratios γ of ^{7}Li and ^{6}Li are 10.3976×10^7 and 3.9371×10^7 rad T^{-1} s^{-1}, respectively).[11] Therefore the fluorine resonance of a species with coupled lithium and fluorine atoms should be broader for molecules with ^{7}Li than for molecules with ^{6}Li. We conclude that the additional resonance at δ -197 ppm originates from such lithium fluoride species. The resonance was also present in the spectrum taken after one week.

Competition experiment for solvation of **5** with deuterated trichloromethane and deuterated tetrahydrofuran were carried out by adding $CDCl_3$ to a THF-d_8 solution of **3**·2THF (Fig. 3f–h). In contrast to the solution of **3**·2THF in $CDCl_3$, the formation of **1** was not observed. Fluorine resonances of both deuterated trichloromethane (**5**·$CDCl_3$) and tetrahydrofuran (**5**·THF/**5**·2THF) solvated monomeric species were observed in the temperature range of 220 to 250 K in a 0.007 M solution of **3**·2THF in $CDCl_3$/THF-d_8 (molar ratio 2.5 : 1). The fluorine resonances almost completely broaden into the baseline at 280 K. The ratio of deuterated trichloromethane-solvated to tetrahydrofuran-solvated species is approximately 1 at 220 K and 0.5 at 250 K, which indicates similar solvation free-energies of lithium ion in **5** by both deuterated trichloromethane and tetrahydrofuran. The broadening of resonances at 280 K suggests a facile exchange of both solvating molecules on lithium ion.

The high-frequency shift of F_a resonances of **5**·$(THF)_x$ and **5**·$CDCl_3$ was observed at higher temperature in $CDCl_3$/THF-d_8 solution of **3**·2THF (Fig. 3f–h). The F_a resonance of **5**·$(THF)_x$ shifts to lower frequency (for 40 ppm) after adding $CDCl_3$ to a THF solution of **3**·2THF (Fig. 3c,f). The temperature and solvent dependency of F_a resonances of $[(Cp^*{}_2Ti_2F_7)_2Ca]$ has been reported.[10b] We assume that the solvation of fluorine atoms of $[Cp^*{}_2Ti_2F_7]^-$ ligand is facilitated by F ··· D–CCl_3 hydrogen bonds. The F_a atoms are sterically the most available for solvation and therefore the F_a resonance shows the most pronounced effect of temperature or addition of $CDCl_3$. The addition of $CDCl_3$ to a THF-d_8 solution of **3**·2THF in competition experiment shifts the F_d resonance of **5**·$(THF)_x$ by 10 ppm to higher frequency and F_c resonance by 1 ppm to lower frequency. These different shifts of resonances result in their reversed appearance in a $CDCl_3$/THF-d_8 solution in comparison to a THF-d_8 solution (Fig. 3c,f).

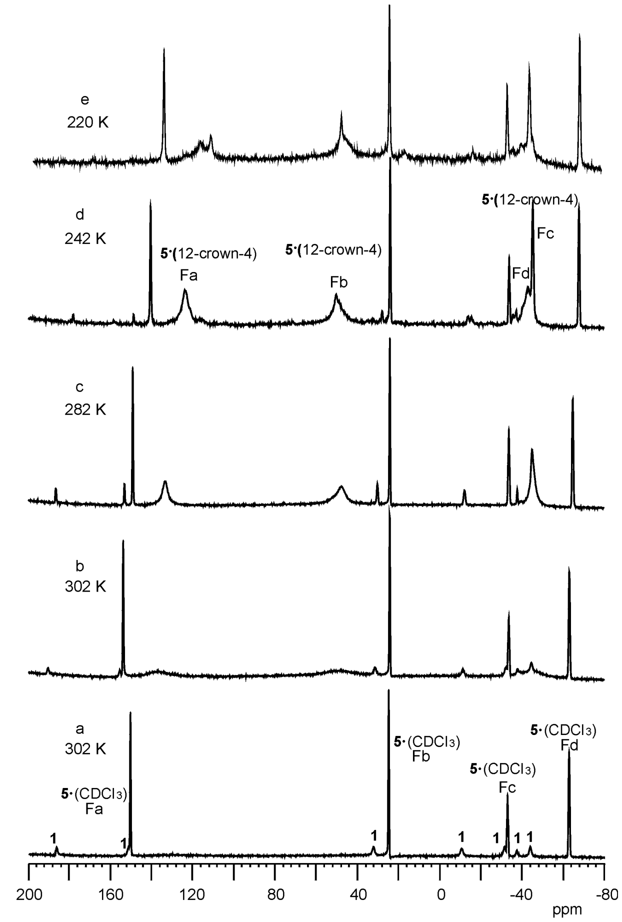

Fig. 5 Variable temperature ^{19}F NMR spectra of **4**·12-crown-4 at 282 MHz; (a) $CDCl_3$ (0.032 M) solution, (b–e) 0.024 M $CDCl_3$/12-crown-4 (molar ratio 8 : 1) solution.

VT NMR spectra of 4·(12-crown-4) in $CDCl_3$ and in $CDCl_3$/12-crown-4. The ^{19}F NMR spectrum of a deuterated trichloromethane solution of 4·(12-crown-4) is very similar to that of **3**·2THF and four resonances in the intensity ratio of 2 : 2 : 1 : 2 are ascribed to **5**·$CDCl_3$ (Fig. 5). Similarly to **3**·2THF, the seven minor resonances of **1** are also observed. The competition experiments for solvation of **5** with deuterochloroform and 12-crown-4 were carried out by adding 12-crown-4 to the $CDCl_3$ solution of 4·(12-crown-4) (Fig. 5b–d). A new set of resonances appeared, which were ascribed to the monosolvated **5**·(12-crown-4). The fluorine resonances of **5**·(12-crown-4) and **5**·$CDCl_3$ were observed in slow exchange up to 302 K. An increase in the concentration ratio of **5**·12-crown-4 to **5**·$CDCl_3$ was observed when the solution was cooled. The equilibrium constants for the exchange of deuterated trichloromethane with 12-crown-4 shown in Scheme 4 were calculated from the intensity ratio of F_a resonances of **5**·(12-crown-4) and **5**·$CDCl_3$.

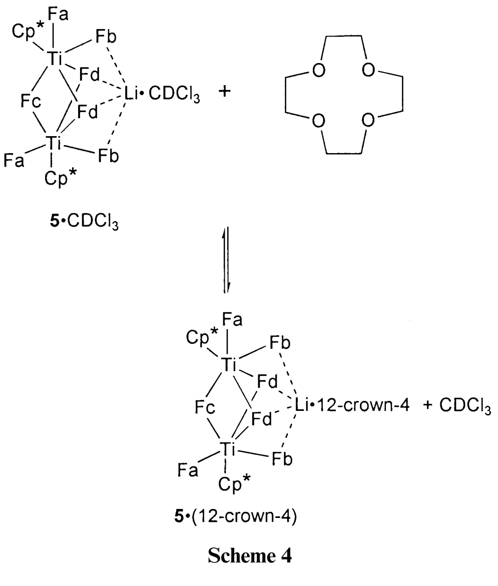

Scheme 4

The equilibrium constants 2.88 (292 K), 3.41 (282 K), 3.76 (272 K), 4.36 (262 K), 4.59 (252 K), 5.24 (242 K) and 5.55 (232 K) resulted in ΔH of −6.0(1) kJ mol^{-1} and ΔS of −30(3) J mol^{-1} K^{-1}. The low negative ΔS suggests that the number of molecules is unchanged by the solvation equilibrium and supports the presence of monosolvated **5**·(12-crown-4) in the solution. The ΔH is comparable to the difference of solvation enthalpies of $[\{(C_5Me_4Et)_2Ti_2F_7\}_2Ca]$ with $CDCl_3$ (−19 kJ mol^{-1}) and with dioxane (−23 kJ mol^{-1}).[9b–c] The **5**·$CDCl_3$ fluorine resonances in the $CDCl_3$/12-crown-4 solution of **4**·(12-crown-4) are not broadened into the baseline as in the case of a $CDCl_3$/THF-d_8 solution of **3**·2THF. The exchange of the solvating 12-crown-4 and $CDCl_3$ molecules on lithium is therefore much slower than the exchange of the solvating $CDCl_3$ and THF-d_8 molecules observed in $CDCl_3$/THF-d_8 solution of **3**·2THF. On the other hand, the fluorine resonances of **5**·(12-crown-4) are broad and an onset of decoalescence of resonances is visible at cooling the solution to 220 K (Fig. 5b–e). In addition, only a single ^1H NMR resonance of 12-crown-4 appears in a competition experiment at low temperature (217 K). Both observations suggest the nonrigidity of **5**·(12-crown-4) possibly by interconversions between monodentate and tetradentate coordination of 12-crown-4 to a lithium atom or by moving of the lithium between donating fluorines of the $[Cp^*{}_2Ti_2F_7]^-$ ligand.

The ^7Li NMR spectra of $CDCl_3$ solutions of **3**·2THF and **4**·(12-crown-4) and ^6Li NMR of $[^6Li]$**3**·2THF show a broad resonance between δ −0.5 and −2.5 ppm. The resonance is broadened presumably due to ^7Li–^{19}F or ^6Li–^{19}F coupling. We were unable to extract additional information on solution behaviour of prepared compounds from ^7Li and ^6Li NMR

Table 3 Optimized distances (in Å) in the structures of $\mathbf{5'}\cdot(OMe_2)$,$\mathbf{5'}\cdot2(OMe_2)$ and $\mathbf{5'}\cdot3(OMe_2)$ at HF/6-31G

Structure	Li–O1	Li–O2	Li–O3	Li–F1	Li–F2	Li–F3	Li–F4
$\mathbf{5'}\cdot(OMe_2)$	1.879	—	—	2.002	2.000	2.030	2.031
$\mathbf{5'}\cdot2(OMe_2)$	1.943	1.954	—	2.115	2.266	2.113	2.108
$\mathbf{5'}\cdot3(OMe_2)$	2.062	2.045	2.041	2.038	3.182	3.366	2.067

spectra due to the broadening of resonances and due to the small range of ^{7}Li and ^{6}Li chemical shifts.[1e]

Theoretical calculations

In order to shed an additional light on the solvation of monomeric species **5** in THF solution, we performed quantum-mechanical calculations. To reduce the calculation time an unsubstituted Cp-ring instead of Cp*, and a dimethyl ether molecule instead of a THF were used. The optimized geometries and distances of $(Cp_2Ti_2F_7)Li(OMe_2)$, $\mathbf{5'}\cdot(OMe_2)$, $(Cp_2Ti_2F_7)Li(OMe_2)_2$, $\mathbf{5'}\cdot2(OMe_2)$ and $(Cp_2Ti_2F_7)Li(OMe_2)_3$, $\mathbf{5'}\cdot3(OMe_2)$ at HF/6-31G level of theory are summarised in Fig. 6 and Table 3. The lithium cation in $\mathbf{5'}\cdot(OMe_2)$ adopts a distorted trigonal-bipyramidal environment with Li–O bonding distance 1.879 Å, two short Li–F distances (2.000 and 2.002 Å) and two slightly longer Li–F distances (2.030 and 2.031 Å). The energy difference for the addition of the second dimethyl ether molecule to $\mathbf{5'}\cdot(OMe_2)$ is calculated to be −13.00 kcal mol^{-1}. The lithium cation in $\mathbf{5'}\cdot2(OMe_2)$ adopts a distorted octahedral environment. The two Li–O bonding distances are not identical (1.943 and 1.954 Å), and are lengthened by 0.06 and 0.07 Å when compared to $\mathbf{5'}\cdot(OMe_2)$. The four Li–F bonding distances are also lengthened, Li–F3 and Li–F4 (2.113 and 2.108 Å) by 0.08 Å and the Li–F1 distance (2.115 Å) by 0.11 Å. The Li–F2 (2.266 Å) is lengthened by the largest amount, the difference being 0.266 Å when compared to $\mathbf{5'}\cdot(OMe_2)$. There are two sets of Li–F bonding distances in the monoetherate complex, while in the dietherate complex there are three sets of Li–F bonding distances, owing to differences between the Li–F1 and Li–F2 bond distances. The transformation of dititanate anion from tetradentate to bidentate ligand occurs at the addition of the third dimethyl ether molecule to $\mathbf{5'}\cdot2(OMe_2)$. The addition is exothermal ($\Delta E = -2.96$ kcal mol^{-1}). The lithium cation in $\mathbf{5'}\cdot3(OMe_2)$ adopts a distorted trigonal-bipyramidal environment with three Li–O bonding distances (from 2.041 to 2.062 Å) and with two Li–F distances (2.038 and 2.067 Å) from dititanate anion $(Cp_2Ti_2F_7)$ acting as a bidentate ligand.

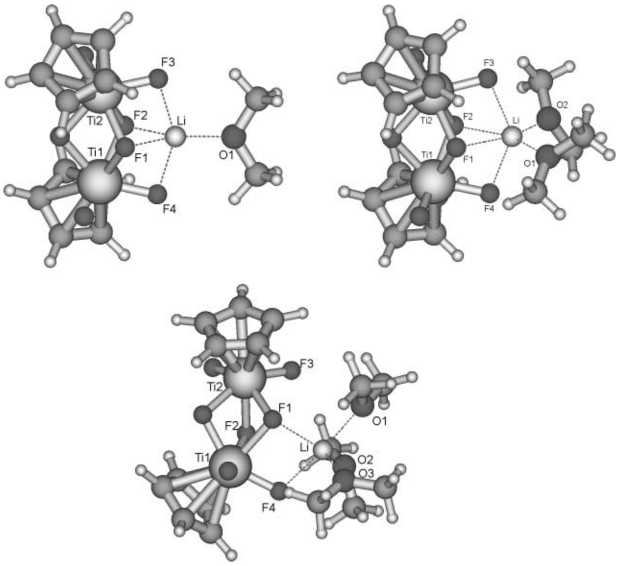

Fig. 6 Optimized structures of $\mathbf{5'}\cdot(OMe_2)$, $\mathbf{5'}\cdot2(OMe_2)$ and $\mathbf{5'}\cdot3(OMe_2)$.

Incremental interaction energies for the introduction of dimethyl ether molecules to $(Cp_2Ti_2F_7)Li$ are −23.46, −13.00 and −2.96 kcal mol^{-1}. These values could be used to get a rough estimate of equilibria of monomeric $\mathbf{5}\cdot(THF)_x$ in THF solution. The energy gain for the addition of the second ether molecule suggests an equilibrium of **5**·THF and **5**·2THF. The formation of **5**·3THF should be entropically disfavoured due to low energy gain.

Conclusion

Two novel lithium complexes, $[\{Li(Cp^*{}_2Ti_2F_7)\}_2(THF)_2]\cdot2THF$ and $[\{Li(Cp^*{}_2Ti_2F_7)\}_2(\mu_2\text{-}\eta^1{:}\eta^1\text{-12-crown-4})]\cdot(12\text{-crown-4})$, were obtained by the treatment of $[Cp^*TiF_3]_2$ with one equivalent of the *in situ* formed LiF. Crystal structure analyses revealed similar structures in both complexes and unusual η^1-coordination of 12-crown-4 to the lithium cation, with the absence of the common η^4-coordination mode of 12-crown-4. ^{19}F NMR was found to be a useful tool for studies of lithium solvation, where slow exchange of deuterated trichloromethane and THF as well as 12-crown-4 on lithium ion was observed in the solution in the temperature range from 170 to 302 K.

Experimental

General

All experimental manipulations were carried out under a nitrogen or argon atmosphere using standard Schlenk techniques or a drybox. Solvents were dried over a Na/K alloy and distilled prior to use. Deuterated NMR solvents were treated with CaH_2, distilled and stored under argon.

NMR spectra were recorded on a Bruker DPX 300 spectrometer operating at 300 MHz (^{1}H), 282 MHz (^{19}F), 116 MHz (^{7}Li) and 44 MHz (^{6}Li). Infrared spectra (Nujol) were recorded on a Perkin-Elmer FT-1720X spectrometer. Elemental analyses were carried out on a Perkin-Elmer 2400 CHN analyser at the University of Ljubljana (Department of Organic Chemistry).

$[Cp^*TiF_3]$[12] and Me_3SnF[13] were prepared according to the literature. 12-Crown-4 was purchased from Aldrich, $[^6Li]\mathbf{3}\cdot2THF$ and $[^6Li]\mathbf{4}\cdot(12\text{-crown-4})$ were prepared using ^{6}LiCl (Campro) instead of LiCl (Kemika).

Synthesis

$[\{Li(Cp^*{}_2Ti_2F_7)\}_2(THF)_2]$ (3). $[(C_5Me_5)TiF_3]_2$ (0.48 g, 1 mmol), Me_3SnF (0.18 g, 1 mmol) and LiCl (43 mg, 1 mmol) were dissolved in THF (50 mL). The orange solution was stirred overnight, and afterwards THF and Me_3SnCl were removed *in vacuo*. The orange–red solid was recrystallized from THF, washed with pentane and dried (0.44 mg, 76% yield). Anal. Calcd for $C_{48}H_{76}F_{14}Li_2O_2Ti_4$: C, 49.85; H, 6.62. Found: C, 49.67; H, 6.62%. ^{1}H NMR (300 MHz, $CDCl_3$): δ 3.74 (m, 8H, THF), 2.15 and 2.10 (two s, 60H, C_5Me_5), 1.85 (m, 8H, THF); ^{19}F NMR (282 MHz, $CDCl_3$): δ 150.8 (qnt, 2F, $^2J_{F-F} = 40$ Hz), 25.2 (s, 2F), −33.0 (m, 1F), −63.4 (s, 2F); ^{7}Li NMR (116 MHz, $CDCl_3$): δ −1.28 (m), −1.95 (m). IR (Nujol) (cm^{-1}): 1262m, 1095m, 804m, 614s, 567vs, 536s, 474m.

$[\{Li(Cp^*{}_2Ti_2F_7)\}_2(\mu_2\text{-}\eta^1{:}\eta^1\text{-12-crown-4})]\cdot(12\text{-crown-4})$ 4·(12-crown-4). **3** (0.51 g, 0.5 mmol) was dissolved in THF (30 mL), followed by the addition of 12-crown-4 (0.70 g, 4 mmol) followed. The orange solution was stirred overnight. Orange–red crystals of **4**·(12-crown-4) were grown from the solution at 4 °C

Table 4 Crystal and refinement data for complexes **3**·2THF and **4**·(12-crown-4)

Complex	**3**·2THF	**4**·(12-crown-4)
Empirical formula	$C_{56}H_{92}F_{14}Li_2O_4Ti_4$	$C_{56}H_{92}F_{14}Li_2O_8Ti_4$
M	1300.78	1364.78
Crystal system	Triclinic	Monoclinic
Space group	$P\bar{1}$ (no. 2)	$P2_1/n$ (no. 14)
a/Å	11.0247(2)	11.2521(2)
b/Å	12.1616(2)	15.3194(3)
c/Å	13.8922(3)	18.6121(3)
a/°	66.9190(10)	90.00
β/°	87.9420(10)	101.4240(10)
γ/°	65.1930(10)	90.00
V/Å^3	1536.88(5)	3144.71(10)
T/K	150	190
Z	1	2
μ/mm^{-1}	0.585	0.580
Data measured, unique (R_{int})	11959, 6815 (0.0283)	12796, 6762 (0.0187)
R,[a] wR_2[b] [I>2σ(I)]	0.0397, 0.0911	0.0511, 0.1405
R, wR_2 (all data)	0.0569, 0.0993	0.0616, 0.1518

[a] $R = \Sigma| |F_o| - |F_c||/\Sigma|F_o|$. [b] $wR_2 = \{\Sigma[w(F_o^2 - F_c^2)^2]/ \Sigma[w(F_o^2)^2]\}^{1/2}$. [c] $S = \{\Sigma[w(F_o^2 - F_c^2)^2]/(n - p)\}^{1/2}$, where n is the number of reflections and p is the total number of parameters refined.

(0.42 mg, 62% yield). Anal. Calcd for $C_{56}H_{92}F_{14}Li_2O_8Ti_4$: C, 49.29; H, 6.80. Found: C, 48.37; H, 6.91%. ^{1}H NMR (300 MHz, $CDCl_3$) δ 3.70 (s, 32H, 12-crown-4), 2.14 and 2.10 (two s, 60H, C_5Me_5); ^{19}F NMR (282 MHz, $CDCl_3$): δ 148.3 (qnt, 2F), 24.9 (s, 2F), −32.5 (m, 1F), −62.3 (s, 2F); ^{7}Li NMR (116 MHz, $CDCl_3$): δ −1.51, −1.95 (overlapping m). IR (Nujol) (cm^{-1}): 1309s, 1254s, 1131vw, 928s, 850s, 804m, 604s, 540s, 477s, 406s.

X-Ray crystallography

Crystal data and refinement parameters for **3**·2THF and **4**·(12-crown-4) are listed in Table 4. Selected crystals of **3**·2THF and **4**·(12-crown-4) were quickly mounted on glass fibers and placed in a stream of cold nitrogen. Data were collected on a Nonius Kappa CCD diffractometer equipped with a Mo anode (Kα radiation, λ = 0.71073 Å) and graphite monochromator. The structures were solved by direct methods (SHELXS-97)[14] and refined by a full-matrix least-squares procedure based on F^2 (SHELXL-97).[15] All non-hydrogen atoms were refined anisotropically, while the hydrogen atoms were included in the model at geometrically calculated positions and refined using a riding model.

CCDC reference numbers 191337 and 185829.

See http://www.rsc.org/suppdata/dt/b2/b207685c/ for crystallographic data in CIF or other electronic format.

Computational details

Full geometry optimisations with no symmetry constraints were performed at the Hartree–Fock level of theory using the 6-31G standard basis set for all elements. Calculations were carried out using GAUSSIAN-98 set of programs.[16]

Acknowledgements

This work was supported by the Grants PO-0511–0103 and PO-0503–0103 from the Ministry of Education, Science and Sport, Republic of Slovenia and by the Deutsche Forschungsgemeinschaft. F. P. is grateful to Dr. J. Mavri and Mr. J. Stare, National Institute of Chemistry, Slovenia, for fruitful discussions.

References

1 A few recent examples: (*a*) G. W. Klumpp, *Recl. Trav. Chim. Pays-Bas*, 1986, **105**, 1; (*b*) S. T. Chadwick, R. A. Rennels, J. L. Rutherford and D. B. Collum, *J. Am. Chem. Soc.*, 2000, **122**, 8640; (*c*) F. Haeffner, C. Z. Sun and P. G. Williard, *J. Am. Chem. Soc.*, 2000, **122**, 12542; (*d*) K. W. Henderson, A. E. Dorigo, P. G. Williard and P. R. Bernstein, *Angew. Chem., Int. Ed. Engl.*, 1996, **35**, 1322; (*e*) D. Hoffmann, A. Dorigo, P. v. R. Schleyer, H. Reif, D. Stalke, G. M. Sheldrick, E. Weiss and M. Geissler, *Inorg. Chem.*, 1995, **34**, 262; (*f*) D. Hoffmann and D. B. Collum, *J. Am. Chem. Soc.*, 1998, **120**, 5810; (*g*) H. J. Reich, J. P. Borst, R. R. Dykstra and D. P. Green, *J. Am. Chem. Soc.*, 1993, **115**, 8728; (*h*) H. J. Reich and K. J. Kulicke, *J. Am. Chem. Soc.*, 1996, **118**, 273.

2 B. L. Lucht and D. B. Collum, *Acc. Chem. Res.*, 1999, **32**, 1035.

3 R. K. Harris and P. Jackson, *Chem. Rev.*, 1991, **91**, 1427.

4 A. Demšar, A. Pevec, L. Golič, S. Petriček, A. Petrič and H. W. Roesky, *Chem. Commun.*, 1998, 1029.

5 M.-L. Lehaire, R. Scopelleti, H. Piotrovski and K. Severin, *Angew. Chem., Int. Ed.*, 2002, **41**, 1419.

6 A. F. Wells, *Structural Inorganic Chemistry*, Clarendon Press, Oxford, UK, 4th edn., 1975, p. 375.

7 (*a*) J. W. Steed, *Coord. Chem. Rev.*, 2001, **215**, 171; (*b*) R. M. Izatt, K. Pawlak, J. S. Bradshaw and R. L. Bruening, *Chem. Rev.*, 1991, **91**, 1721.

8 T. Akutagawa, T. Nakamura, T. Inabe and A. E. Underhill, *J. Mater. Chem.*, 1997, **7**, 183.

9 (*a*) F. Perdih, A. Demšar, A. Pevec, S. Petriček, I. Leban, G. Giester, J. Sieler and H. W. Roesky, *Polyhedron*, 2001, **20**, 1967; (*b*) F. Perdih A. Demšar A. Pevec and S. Petriček, manuscript in preparation.

10 (*a*) A. Pevec, A. Demsar, V. Gramlich, S. Petricek and H. W. Roesky, *J. Chem. Soc., Dalton Trans.*, 1997, 2215; (*b*) A. Demšar, A. Pevec, S. Petriček, L. Golič, A. Petrič, M. Bjorgvinsson and H. W. Roesky, *J. Chem. Soc., Dalton Trans.*, 1998, 4043; (*c*) A. Demšar, F. Perdih, A. Petrič, A. Pevec and S. Petriček, *Acta Chim. Slov.*, 1999, **46**, 185.

11 B. E. Mann, in *Encyclopedia of Inorganic Chemistry*, ed. R. B. King, Wiley, New York, 1994, vol. 5, pp. 2615–2645.

12 (*a*) A. Herzog, F.-Q. Liu, H. W. Roesky, A. Demšar, K. Keller, M. Noltemeyer and F. Pauer, *Organometallics*, 1994, **13**, 1251; (*b*) M. Schormann, H. W. Roesky, M. Noltemeyer and H.-G. Schmidt, *J. Fluorine Chem.*, 2000, **101**, 75; (*c*) M. Sootodeh, I. Leichtweis, H. W. Roesky, M. Noltemeyer and H.-G. Schmidt, *Chem. Ber.*, 1993, **126**, 913.

13 E. Krause, *Ber. Dtsch. Chem. Ges.*, 1918, **51**, 1447.

14 G. M. Sheldrick, SHELXS-97, A program for automatic solution of crystal structures, University of Göttingen, Göttingen, Germany, 1997.

15 G. M. Sheldrick, SHELXL-97, A program for crystal structure refinement, University of Göttingen, Göttingen, Germany, 1997.

16 M. J. Frisch, G. W. Trucks, H. B. Schlegel, G. E. Scuseria, M. A. Robb, J. R. Cheeseman, V. G. Zakrzewski, J. A. Montgomery, Jr., R. E. Stratmann, J. C. Burant, S. Dapprich, J. M. Millam, A. D. Daniels, K. N. Kudin, M. C. Strain, O. Farkas, J. Tomasi, V. Barone, M. Cossi, R. Cammi, B. Mennucci, C. Pomelli, C. Adamo, S. Clifford, J. Ochterski, G. A. Petersson, P. Y. Ayala, Q. Cui, K. Morokuma, D. K. Malick, A. D. Rabuck, K. Raghavachari, J. B. Foresman, J. Cioslowski, J. V. Ortiz, A. G. Baboul, B. B. Stefanov, G. Liu, A. Liashenko, P. Piskorz, I. Komaromi, R. Gomperts, R. L. Martin, D. J. Fox, T. Keith, M. A. Al-Laham, C. Y. Peng, A. Nanayakkara, C. Gonzalez, M. Challacombe, P. M. W. Gill, B. Johnson, W. Chen, M. W. Wong, J. L. Andres, C. Gonzalez, M. Head-Gordon, E. S. Replogle and J. A. Pople, *GAUSSIAN-98, Revision A.7*, Gaussian, Pittsburgh, PA, 1998.